NEW PROCESSOR AND REFERENCE DATASET FOR HYPERSPECTRAL CHRIS-PROBA IMAGES OVER COASTAL AND INLAND WATERS

Héloïse Lavigne[1], Quinten Vanhellemont[1], Kevin Ruddick[1], Ana Dogliotti[2]

1. Royal Belgian Institute of Natural Sciences (Brussels, Belgium)
2. Instituto de Astronomía y Física del Espacio (Buenos Aires, Argentina)

ABSTRACT

Hyperspectral remote sensing is expected to facilitate aquatic applications, such as the monitoring of harmful algal blooms or the determination of suspended sediment properties. However, this requires accurate processing to retrieve water reflectance from top of atmosphere radiance. Here we present a new processor for hyperspectral (mode 1) CHRIS-PROBA images and make available to the public a sample dataset of water reflectance images. Although the CHRIS-PROBA sensor has been operating for about 20 years, only a few images with water targets were acquired with the hyperspectral mode (mode 1) and a dedicated atmospheric correction was needed. The processor presented here includes systematic noise removal, atmospheric correction and georeferencing. Validation of water reflectance products shows generally good consistency between in situ and satellite measurements although an underestimation in the 400 nm – 470 nm range was observed. Finally, it is expected that the sample dataset of hyperspectral water reflectance images will be useful to test new algorithms for water products or to compare processing methods.

Index Terms— hyperspectral, CHRIS-PROBA, water reflectance, atmospheric correction

1. INTRODUCTION

Hyperspectral remote sensing is expected to facilitate new aquatic applications such as the monitoring of harmful algal blooms, improved detection of macro-algae and floating vegetation, and the determination of suspended sediment properties in coastal and inland waters.

Although many hyperspectral sensors are currently in development (i.e. PACE), under construction (i.e. ENMAP) or have been recently launched (i.e. DESIS, PRISMA), several others have been acquiring data for previous years, providing an important database to test processing and algorithms. Among these historical sensors one can mention HYPERION [1] and HICO [2] which operated respectively from 2009 to 2017 and from 2010 to 2014, and the CHRIS-PROBA sensor [3] which was launched in 2001 and is still operational. CHRIS-PROBA is a programmable sensor with different acquisition modes representing a trade-off between spatial, spectral and radiometric resolution. The capability of CHRIS-PROBA was already demonstrated over land and waters ([3], [4], [5]). However, for water targets, it was recommended to use acquisition mode 2 (increased gain; multispectral) and very little is known about CHRIS hyperspectral (mode 1) performance over coastal and inland waters. To test CHRIS hyperspectral capabilities for aquatic applications, we first retrieved water reflectance from CHRIS images over selected coastal and inland water test sites. The water reflectance products can then be used for testing hyperspectral algorithms, e.g. to derive additional information on water particles. Here we present the atmospheric correction and processing developed for hyperspectral CHRIS images and the validation of the resulting products. A previous atmospheric correction algorithm designed for land, based on vegetation similarity spectrum, has been produced for CHRIS images [3] but to improve results over water targets we developed a new processing based on the Dark Spectrum Fitting (DSF) approach [6]. Finally, a sample dataset of Level 2 water reflectance products is produced and described here. This dataset is shared in open access to allow other users to test hyperspectral algorithms for water products.

2 METHOD

2.1. CHRIS-PROBA image acquisition

3. CHRIS-PROBA images were acquired in mode 1 with multi-view option. Mode 1 CHRIS images contain 62 spectral bands between 400 nm and 1000 nm with about 10 nm band width. CHRIS images are 13x13 km square images with 36 m spatial resolution. With multi-view acquisition, in the best case, 5 images are acquired within <2.5 min. These images are defined using their Fly by Zenith Angle (FZA): -55°, -36°, 0°, 36° and 55°. The FZA angle is defined as the zenith angle between the platform and the "fly-by" target (i.e. the point of the ground projected track corresponding to the minimum zenith viewing angle [7]). Level 1 HDF CHRIS files were downloaded from the ESA server (https://tpm-ds.eo.esa.int/smcat/PROBA1-CHRIS/0/0/0/). They were all processed with the version 4.1 of the ESA CHRIS processor for Level 1a, which was updated in 2008 [8].

Over the period 2018-2020, 96 multi-view (i.e. 5 replicates) CHRIS_PROBA images were acquired for 10 different geographic sites over coastal and inland waters and for two open water sites. Open water sites were used for inter-band calibration ([8], [9]).

2.2. Image processing

To process a level 1 CHRIS-PROBA image to water reflectance, a new processing chain was designed. It includes four successive modules for data pre-processing, (1) vertical striping correction, (2) inter-band calibration, (3) atmospheric correction and (4) geolocation. CHRIS-PROBA top of atmosphere (TOA) radiance data provided in Level 1 products are rather noisy. However, this noise is only partially caused by standard random noise as it also contains a deterministic disturbance pattern due to the generation of the image by the CHRIS instrument [10]. For vertical striping correction the algorithm proposed by [10] was applied and an additional algorithm was developed to correct remaining coherent patterns in small-scale inter-band variability [11].

Atmospheric correction is based on the DSF method [6]. The DSF assumes that atmospheric aerosol composition and density is homogeneous over the image or the sub-scene processed and that for at least one spectral band and one pixel the surface reflectance is null (hereafter dark pixel). As DSF has been validated for Landsat-8 and Sentinel-2 with sensors that have similar spatial resolution to CHRIS, it is realistic to assume that these conditions will also be valid for CHRIS-PROBA images. The CHRIS-PROBA DSF version was slightly simplified by fixing the aerosol model to the maritime model. Dark pixels are extracted for spectral bands between 500 nm and 970 nm, excluding bands impacted by gas absorption peaks (oxygen, water vapor, ozone). The DSF is applied twice. In the first step, DSF is applied individually to each CHRIS-PROBA image with different viewing geometry to derive a set of five aerosol optical thickness (AOT) values. As the five CHRIS-PROBA images are taken in a short period of time (<2.5 min) and over a small spatial area, we suppose that aerosol properties should be the same for the different viewing angles. Hence, similarly to [12], we consider the lowest AOT value among angles FZA =-36°, FZA=0° and FZA=36° to be the best estimation of AOT. Indeed, for low to medium zenith angle, sunglint is one of the main phenomena impacting the bi-directional reflectance function (BRDF) which results in an overestimation of AOT. High zenith angles (FZA=55° and FZA = -55°) were excluded because they present higher uncertainties due to long optical path and strong Fresnel reflectance at the water surface. In the second step, the five CHRIS-PROBA images were reprocessed with DSF but with a fixed and identical AOT value.

Finally, as CHRIS-PROBA images are not provided with latitude and longitude fields, a georeferencing was performed with the SNAP software (https://step.esa.int/main/toolboxes/snap/) using at least 5 ground control points identified as particular features of the images and interpolation based on linear polynomial method. This procedure allowed to produce latitude and longitude fields with an average level of uncertainty of 0.003°.

3. RESULTS AND DISCUSSION

3.1. Validation

Three valid in situ / CHRIS-PROBA hyperspectral matchups were available in the period 2018-2020: one from Lake Chascomus (-35.5839°N, -58.0212°E) on 2019-03-21 and two in spring/summer 2020 from a hyperspectral TriOS sensor integrated to an autonomous measurement system (PANTHYR, [13]) deployed on the blue accelerator platform (https://www.blueaccelerator.be/). This platform is located ~500 meters outside the port of Ostend (51.2464°N, 2.9193°E) where the PANTHYR performed autonomous measurements every 20 minutes for about 9 months. For all match-ups, a time window of +/- 30 minutes between in situ and satellite measurements was used.

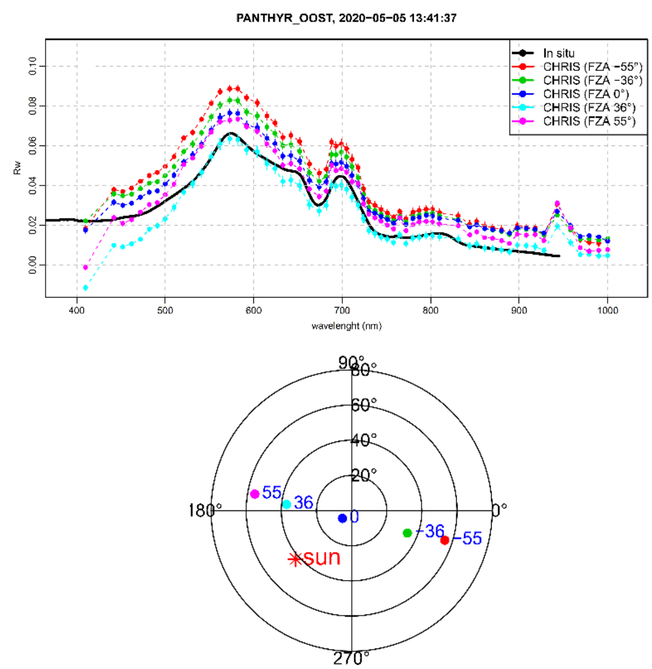

Figure 1. Spectral comparison of in situ water reflectance measurements (black line) and simultaneous CHRIS-PROBA spectra. Colours refer to CHRIS acquisition geometry which is represented on polar graphic and defined with the Fly by Zenith angle. On polar graphic zenithal angle is represented by radius.

Comparison of in situ and CHRIS spectra for the Ostend matchup on 2020-05-05 shows consistent results in term of shape of the spectra. However, as also observed by [3] an important directional pattern is displayed with a large overestimation of water reflectance for certain geometry although no direct sunglint was expected. Images taken away from the sun (FZA=36° or FZA=55° on Figure1) show lower reflectances that better match in situ observations than images taken with a geometry closer to the specular position of the sun (FZA = -36°) and images with high view zenith angles (FZA = 55° and FZA = -55°). Although, this pattern is only presented for one match-up on Figure 1 it was observed in the three available match-ups, and hence we selected only images with FZA = +/- 36° with an azimuth angle viewing away from the sun for quantitative validation and further analyses.

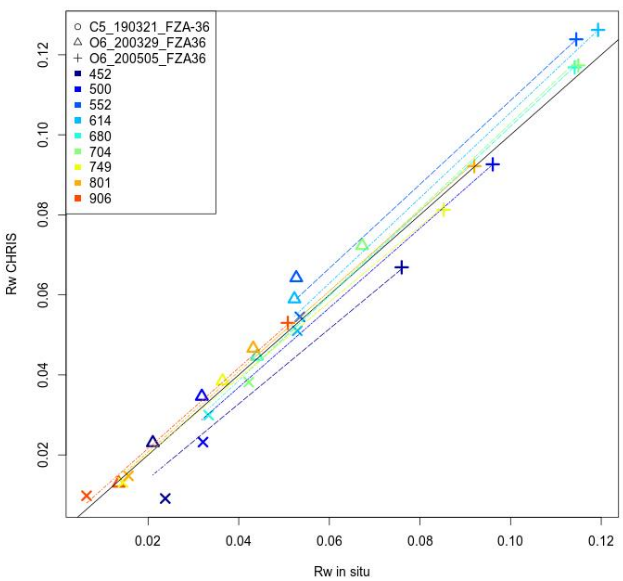

Figure 2: In situ water reflectance at the Ostend (O6) and Chascomus (C5) sites as a function of CHRIS-PROBA reflectance for selected wavelengths. Dotted lines represent linear regression calculated for each band. Colours refer to spectral bands and symbol shape to different images (see legend).

Figure 2 shows a scatter plot between in situ and CHRIS-PROBA water reflectance for selected wavelengths. As only three datapoints are available for each band, these results presented in Figure 2 should be interpreted with caution. Overall, a positive relationship is observed with a slope close to 1. However, it seems that CHRIS reflectance tends to underestimate and overestimate *in situ* measurements in the 450 - 500 nm and 550 - 614 nm intervals, respectively. This was confirmed by the analysis of the spectral median ratio, which ranged from 0.8 to 1 in the 450 - 500 nm interval and between 1 and 1.15 in the 510 - 615 nm interval. In the 650-904 nm range, a very good coherence between CHRIS and in situ data is observed. The spectral analysis of the median absolute present difference (MAPD) confirmed previous findings: MAPD were <10% between 560 and 700 nm and 10 - 15% in the 450 - 560 nm range. Finally, MAPD was extremely high (about 50%) at 412 and 443 nm and for wavelength between 900 nm and 1000 nm. The high relative errors at these wavelengths are caused by the difficult atmospheric correction and low target signal, but could also be impacted by the radiometric calibration of CHRIS. It should be noted that the calibration of CHRIS was last updated in 2008, more than a decade before these images were acquired ([8], [9]).

3.2. Sample Level 2 dataset

Although Level 2 CHRIS products need to be used with caution due to the underestimation in the 400 nm – 470 nm range, they still have great potential for certain applications. A sample dataset of Level 2 hyperspectral CHRIS-PROBA images was produced with the new processor described in section 2 and is made freely available (ftp://ftp.rbins.be/heloise/IGARSS2021_DATA_SUP/L2_CHRIS_sample_dataset_IGARSS2021.zip). This dataset includes 13 water reflectance images from 10 different test sites in coastal and inland waters with very different properties (see Table 1). Data are provided as NetCDF files and to avoid any confusion only the best CHRIS-PROBA viewing geometry (i.e. FZA=36° or FZA=-36°) is provided in the sample dataset. This data is provided for testing of new algorithms for water applications or to compare processing methods.

Table 1: List of images available in the L2 CHRIS sample database available from: ftp://ftp.rbins.be/heloise/IGARSS2021_DATA_SUP/L2_CHRIS_sample_dataset_IGARSS2021.zip.

Site name	code	date	latitude	longitude
Chascomus	C5	2018-03-19	-35.58°N	-58.02°E
Chascomus	C5	2019-03-21	-35.58°N	-58.02°E
Le-Verdon	J4	2018-09-07	45.55°N	-1.04°E
Nice	N9	2018-10-22	43.65°N	7.20°E
Ostend	O6	2018-05-04	51.24°N	2.92°E
Ostend	O6	2020-05-05	51.24°N	2.92°E
Port-St-Louis	P5	2018-09-01	43.32°N	4.88°E
Pauillac	P6	2018-09-08	45.20°N	-0.74°E
Shanghai	Q3	2018-10-29	31.47°N	121.77°E
Thornton	T6	2019-04-04	51.53°N	2.95°E
Buenos-Aires	U2	2019-01-11	-34.56°N	-58.40°E
Buenos-Aires	U2	2020-03-01	-34.56°N	-58.40°E
Zeebrugge	Z5	2018-08-31	51.35°N	3.17°E

4. CONCLUSION

A dataset of hyperspectral water reflectance CHRIS-PROBA images was produced with a dedicated processor based on the DSF atmospheric correction. Results were validated against in situ measurements and show an overall good performance with a good reproduction of the spectral shape. A significant underestimation of reflectance was observed in the blue bands (400 nm to 470 nm). As CHRIS-PROBA products were not updated with new calibration since 2008 (>12 years), it is not clear whether this underestimation is caused mainly by imperfect atmospheric correction or by calibration problems. A very good accuracy was retrieved for bands between 560 nm and 700 nm (MAPD >10%). Finally, the image dataset is made available to the community, and could be useful to test algorithms for different applications such as the presence/absence of certain phytoplankton species.

5. AKNOWLEDGEMENTS

This work has been funded by BELSPO through the Support To Exploitation and Research in Earth Observation (STEREO)_III HYPERMAQ project (contract nr SR/00/335). We are also very grateful to the European Space Agency (ESA) for acquiring and proving CHRIS-PROBA images and to VLIZ and POM for managing the Ostend validation site.

6. REFERENCES

[1] S. Ungar, J. Pearlman, J. Mendenhall, and D. Reuter. "Overview of the earth observing one (EO-1) mission." *IEEE Transactions on Geoscience and Remote Sensing*, 41(6), 1149-1159, 2003.

[2] M. Corson, D. Korwan, R. Lucke, W. Snyder, and C. Davis. "The hyperspectral imager for the coastal ocean (HICO) on the international space station." *In IGARSS 2008-2008 IEEE International Geoscience and Remote Sensing Symposium* (Vol. 4, pp. IV-101). July 2008.

[3] L. Guanter, L. Alonso, and J. Moreno. "First results from the PROBA/CHRIS hyperspectral/multiangular satellite system over land and water targets". *IEEE Geoscience and Remote Sensing Letters*, 2(3), 250-254, 2005.

[4] G. Casal, T. Kutser, J. Domínguez-Gómez, N. Sánchez-Carnero, and J. Freire, J. "Mapping benthic macroalgal communities in the coastal zone using CHRIS-PROBA mode 2 images." *Estuarine, Coastal and Shelf Science*, 94(3), 281-290, 2011.

[5] S. Mannheim, K. Segl, B. Heim, and H. Kaufmann. "Monitoring of lake water quality using hyperspectral CHRIS-PROBA data." *In Proc. of the 2nd CHRIS/PROBA Workshop* (pp. 28-30), April 2004.

[6] Q. Vanhellemont, Q. "Adaptation of the dark spectrum fitting atmospheric correction for aquatic applications of the Landsat and Sentinel-2 archives". *Remote Sensing of Environment*, 225, 175-192, 2019.

[7] L. Alonso, and J. Moreno. "Quasi-automatic geometric correction and related geometric issues in the exploitation of CHRIS/PROBA data". *In Proceedings* of the second CHRIS/Proba Workshop (pp. 28-30), April 2004.

[8] M. Cutter, and L. Johns. "CHRIS data products–latest issue". In *Proceedings of 3rd CHRIS/Proba Workshop*, ESA/ESRIN, Frascati, June 2005.

[9] M. Cutter. "CHRIS data format". *Surrey Satellite Technology Limited.* document number: SmarTeam #0114848. 2008

[10] L. Gómez-Chova, L. Alonso, L. Guanter, G. Camps-Valls, J. Calpe, and J. Moreno. "Correction of systematic spatial noise in push-broom hyperspectral sensors: application to CHRIS/PROBA images". *Applied Optics*, 47(28), F46-F60, 2008.

[11] H. Lavigne and K. Ruddick. "Inter-band calibration for hyperspectral water remote sensing: demonstration for CHRIS-PROBA". *In proceedings of the IGARSS 2021 meeting*, submitted.

[12] T. Harmel and M. Chami. "Estimation of the sunglint radiance field from optical satellite imagery over open ocean: Multidirectional approach and polarization aspects". *Journal of Geophysical Research: Oceans*, 118(1), 76-90. 2013.

[13] D. Vansteenwegen, K. Ruddick, A. Cattrijsse, Q. Vanhellemont, and M. Beck. "The pan-and-tilt hyperspectral radiometer system (PANTHYR) for autonomous satellite validation measurements—Prototype design and testing." *Remote Sensing*, 11(11), 1360, 2019.